

Displacement and gravity anomaly produced by a shallow vertical dyke in a cohesionless medium

M. Bonafede and M. Olivieri

Dipartimento di Fisica–Settore Geofisica, 8 Viale Berti Pichat, 40127 Bologna, Italy

Accepted 1995 May 15. Received 1995 March 4; in original form 1994 February 14

SUMMARY

A crack model is presented for modelling magma emplacement within a shallow vertical dyke in a half-space which responds elastically in compression but has vanishing tensile strength. Realistic initial stress profiles in the solid rock are considered, corresponding to lithostatic and sedimentary equilibria, while the magma is assumed to possess higher density than the host rock and to conform to the hydrostatic pressure gradient. Equilibrium crack width and extension are computed for several sets of model parameters and, from these, uplift and gravity anomaly at the ground surface. It is shown that, within the model's assumptions, narrow gravity anomalies and uplift can be generated, reaching 50 μgal and 1 m, respectively, provided that the dyke top is very shallow and its vertical extension is large enough (~ 3 km). Dyke injection is accompanied by increasing compression in the host rock at depth, but tensile contributions are generated at shallower depths, around the magma-filled upper portion of the crack, which may play an important role in driving the flow of fluids permeating the upper crust. If the dyke propagates to a shallow enough depth, its uppermost part may remain empty of magma.

Key words: cracks, gravity anomalies, magma flow, uplift.

INTRODUCTION

Intrusion of magma inside the crust is often described in terms of a static tensile crack opening under the overpressure of a filling fluid (e.g. Pollard *et al.* 1983). The governing equation in this case is the stress balance between crack, fluid and host rock.

A few cases of propagating tensile cracks have been also considered (e.g. Spence & Turcotte 1985; Lister 1990, 1991), in which the flow of magma plays an important role, and it is shown that the crack width and the growth speed also depend on fluid dynamics. The propagating problem is, however, much more complex since the crack equation is non-linearly coupled with fluid flow through the lubrication equation, so that analytical solutions can be obtained only under simplifying assumptions (self-similarity or steady state); in particular, these solutions are valid only in unbounded media, i.e. far from the Earth's surface, and cannot be employed to infer characteristics of dyke injection from surface observations. We shall restrict our attention to static models.

Pollard *et al.* (1983) have analysed a few static cases of vertical and oblique cracks under the Earth's surface, addressing their attention to the superficial displacement induced by the crack. Their solutions partially reproduce the surface deformation data obtained during dyke injection episodes at

Kilauea (Hawaii) and Krafla (Iceland) volcanoes. The same model has been applied to recent deformation episodes on Mt Etna (Italy), where microgravity measurements were also available (Murray 1990, 1994; Rymer *et al.* 1993; Budetta, Grimaldi & Luongo 1989, 1990). In all the cases mentioned, the model fails to explain the large ground subsidence (reaching to 20 cm) observed above the presumed dyke location. The numerical models by Pollard *et al.* and by Dieterich & Decker (1975) provide some small subsidence along the strike of a nearly vertical dyke, but this is much smaller than observed and can be shown to depend on the small dimensions of the computational domain (Danesi 1994).

It has been suggested that the failure of crack models to reproduce the observed subsidence is due to the non-elastic behaviour of the medium above the dyke, where tensile stresses are large, but we shall show that no subsidence is provided even if the medium is tensionally non-cohesive.

It should be mentioned that the solution presented in Pollard & Holzhausen (1979) for the vertical component of displacement, while providing large central subsidence, does not vanish at a large distance from the dyke, where it is comparable to the central subsidence. This leads to the conclusion that a rigid body translation, which is not resolvable from the elastostatic equilibrium equations, is entirely responsible for it.

Finally, previous solutions generally assume a constant

overpressure profile inside the crack, while this profile is governed, in the static case, by a gradient related to the density contrast between fluid and host rock.

At great depth within a basaltic crust, magma is lighter than the host rock, because of the higher temperature and the implicitly presumed uniform state and composition, but nearer to the surface, magma density is generally greater than the host volcano-sedimentary rock. This statement is confirmed by the positive gravity anomaly detected, for example, on Mt Etna, in connection with the 1989 and the 1991–1993 eruptions (Budetta *et al.* 1990; Rymer *et al.* 1993). In the latter case, an elongated strip of gravity anomaly of the order of 100 μgal was detected which anticipated by several months the ground deformation and the 1991–1993 eruption; such an anomaly would be compatible with the emplacement of magma within a previously empty shallow dyke, 4 m wide (i.e. $\Delta\rho = \rho!$). Indeed, if we consider that the shallow layers in a volcanic region are mainly formed through volcano-sedimentary processes, such as sequences of ash falls and lava flows, we easily conclude that such layers can be much less dense than the basaltic magma, due to the larger porosity, vesicularity and the presence of open cracks and fissures, related to thermal contraction.

Even from a fracture-mechanical point of view, it would be difficult to treat cases in which $\Delta\rho$ is everywhere negative, since in such a case it would be impossible to stop dyke propagation once it started: according to the Irwing criterion, a tensile crack propagates when the stress intensity factor K is greater than a critical value K_c (a material property), and K increases with increasing length of the crack if the overpressure is everywhere positive within it. If $\Delta\rho < 0$, then any crack-like dyke should always reach the ground surface, once started, since both the increasing buoyancy force and crack length would favour catastrophic propagation.

Lister (1991) employs the Irwing criterion in a steady-state crack model and reaches the same conclusion that, at equilibrium, the upper crack tip must be within the positive $\Delta\rho$ region. He shows the importance of the density stratification in the lithosphere and the related ‘neutral buoyancy level’ (i.e. the depth at which the vertical gradient of magma pressure becomes greater than the gradient of horizontal stress in the host rock). Since $K_c = 0$ in a cohesionless medium, we shall find an even stronger constraint: the crack tip at equilibrium must be shallower than z_{eq} , the depth where magma pressure equals the pre-injection horizontal stress in the host rock.

According to the previous considerations, we shall address our attention to tensile cracks filled with magma with density greater than the host rock; the host rock is assumed to be elastically compressible but with negligible tensional strength. This last property of the medium is chosen for at least three reasons: first, because this is the only way to remove the unrealistic stress singularity at the crack tip; second, because shallow layers in a volcanic edifice, being extensively fractured, are unable to support significant tensional stresses; third, because the assumption of minimum tensile strength for the medium in any case provides a lower bound estimate of the overpressure required for dyke emplacement.

The previous assumptions will help to explain the presence of non-eruptive dykes inside the crust, extensive fissuring of the ground which may not be accompanied by eruptive phenomena, and gravity variations with small amplitudes. Larger gravity variations (sometimes observed) could be also

explained if the density variation within the host rock were significant. However, the large ground subsidence, observed in some instances [e.g. Murray (1994) on Etna, Kanngieser (1983) on Krafla] along the strike of dykes, remains unexplained by any vertical crack model in a homogeneous half-space; it seems plausible that it may be due to shear failure of shallow layers above the dyke, to strong vertical heterogeneities in the host rock or to deflation of a magma reservoir taking place in connection with dyke emplacement.

DESCRIPTION OF THE MODEL

Loosely speaking, we can say that a vertical tensile crack develops in a brittle medium if the normal compressive stress that would act on crack walls from the interior is greater than that originally present in the surrounding medium. In order that the two tractions, from the interior and from the exterior of the fluid–solid interface, may balance, the crack must open so that the compression of the external medium contributes the missing amount of stress. If the crack is filled with a static fluid, the internal stress is given by its pressure, which decreases with hydrostatic gradient from the source region towards the surface. The external stress field, however, is not univocally determined, being controlled by boundary conditions, previous history of emplacement of shallow layers and tectonic contributions. Two extreme cases are considered in the present paper. In the former case the external stress field in the shallow layer is initially lithostatic:

$$\sigma_{xx} = \sigma_{zz} = -\rho_0 g z, \quad (1)$$

where ρ_0 denotes the uniform density of the layer before dyke emplacement, g is gravity, the x -axis is in the horizontal direction, and z is vertically downwards starting from the free surface. The physical convention employed here is that compressive stresses are negative, (however, for ease of understanding, plots will be drawn with reverse orientation on the stress axes). The lithostatic case may be considered as the result of high-temperature emplacement, in which stress becomes isotropic due to the ductile flow of material which completely relieves any deviatoric stress. To this field we may add a tectonic contribution τ_0 in the x -direction,

$$\sigma_{xx} = \sigma_0^L = \tau_0 - \rho_0 g z, \quad (1a)$$

where superscript ‘L’ stands for ‘lithostatic’.

For the latter case considered in the following, it is assumed that the crust is in a sedimentary-like initial state (cold emplacement, with no horizontal displacement), in which case the vertical stress is still determined by the overburden, $\sigma_{zz} = -\rho_0 g z$, while the horizontal component is

$$\sigma_{xx} = \sigma_0^S = \tau_0 - \frac{\nu}{1-\nu} \rho_0 g z, \quad (1b)$$

where ν is the Poisson ratio and superscript ‘S’ stands for ‘sedimentary’. In normal sedimentary processes, a compressive thermoelastic contribution should be added to (1b) due to the long-term readjustment of the geotherm to the new free surface (e.g. Turcotte & Schubert 1982). However, in volcano-sedimentary processes the temperature of deposition is generally greater than the external temperature; hence, the deposited material would undergo short-term cooling before the long-term warming, the overall effect of which could even result in a reversed thermoelastic contribution to the horizontal stress field. In the

following, we shall ignore the thermoelastic contribution, which might be included in τ_0 .

At the base of the dyke, at $z = d$, magma has a pressure p_0 , higher than the horizontal stress $\sigma_{xx}(z = d)$, and density $\rho_m > \rho_0$. According to the initial considerations, the stress σ_m within the dyke is isotropic and has the hydrostatic gradient $-\rho_m g$,

$$\sigma_m = -p_0 - \rho_m g(z - d). \quad (2)$$

The presence of a pressure p_0 , greater than $\sigma_{xx}(z = d)$ (in absolute value), at depth $z = d$, deserves a short digression. As to its origin, magma differentiation processes within a magma chamber, or ascent of hot (hence lighter) magma from the mantle are generally considered to be responsible. We may conceive an initial configuration for the medium in which a layer with density ρ_0 overlays a pressurized magma source. If the overpressure source is 'switched on' after emplacement of the layer ρ_0 , the stress field induced by the overpressure $p_0 - \rho_m g d$ at the source ought to be added to (1a) to obtain the initial stress field; this might be done in a number of ways: for instance, if the magma source, where the overpressure develops, were a sphere of known radius, its stress could be added to the initial configuration (1a) or (1b) employing the available analytical solutions (e.g. Bonafede 1990). It is plausible, however, that only a relatively small, upper region of the magma source is affected by such an overpressure. We prefer to keep the model as simple as possible and accordingly we consider the source region as a lower half-crack (dashed in Fig. 1) where the overpressure builds up gradually from depth $c > d$ up to d , where the lower half-crack merges with the upper half-crack (the dyke).

In the volcano-sedimentary case, there may be another reason why p_0 is greater (in absolute value) than the normal

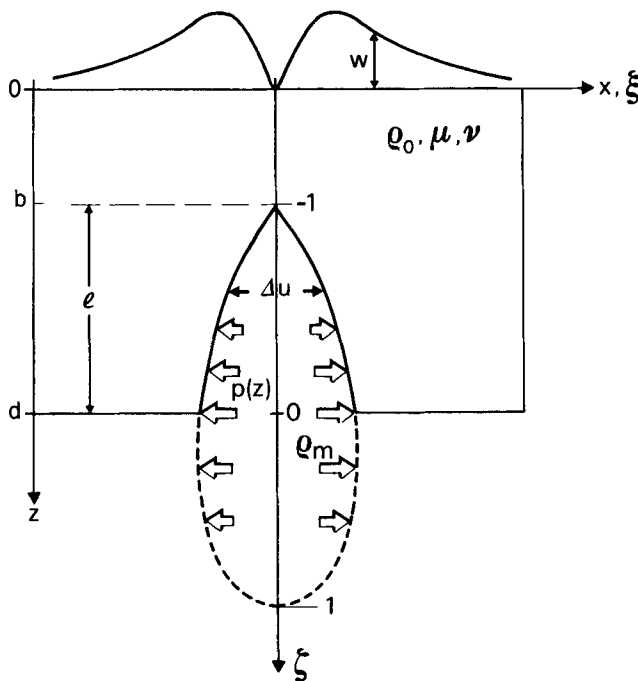


Figure 1. Sketch of the model: the lower half-crack (dashed) is introduced to simulate a magma source region and to produce a closed crack. The z axis is displaced to the left to avoid overlapping of labels with the non-dimensional ξ axis.

stress (1b): this is related to the possible transition from sedimentary equilibrium prevailing in the region $z < d$ to lithostatic equilibrium in the region $z > d$. More specifically, we may conceive of a model in which a sedimentary layer in the region $0 < z < d$, with stress given by (1b), is welded at $z = d$ to a half-space in the region $z > d$ in lithostatic equilibrium, with density ρ_m and isotropic stress $\sigma_{ij} = [(\rho_m - \rho_0)gd - \rho_m g z] \delta_{ij}$. This stress field clearly satisfies the equilibrium equation, the free boundary condition at $z = 0$ and the continuity condition for σ_{zz} at $z = d$. A discontinuity is then present in σ_{xx} at $z = d$. If a magma-filled crack nucleates at $z = d^{(-)}$, the overpressure is $\rho_0 g d - \sigma^S$ (~ 15 MPa if $d = 1$ km, $\nu = 0.25$ and $\tau_0 = 0$). Of course, the transition from sedimentary to lithostatic equilibrium is not sharp in real situations, and the above estimate must be considered as an upper bound.

PRELIMINARIES

The equilibrium configuration for a continuous distribution of tensile dislocations that open under the effect of internal overpressure is governed by the crack equation (e.g. Barenblatt 1962). In a homogeneous, unbounded medium, this equation is a Cauchy-kernel singular integral equation (e.g. Landau & Lifchitz 1967). The solution in a more complex medium (a half-space with a free surface in our case) can be obtained provided that the stress field created by an elementary dislocation with constant slip is known over the dislocation surface (e.g. Erdogan, Gupta & Cook 1973). The solution for an elementary tensile dislocation in a medium composed of two half-spaces, welded over the surface $z = 0$, in which elastic parameters, μ (rigidity) and ν (Poisson modulus), are discontinuous, is provided by Erdogan *et al.* (1973). This solution can be profitably employed in our framework by assuming that the rigidity of the upper half-space (air) vanishes; in this way the upper half-space becomes stress-free. Once this solution is inserted into the crack equation, some non-singular terms are added to the Cauchy kernel. Solving the resulting integral equation, we obtain the distribution of dislocations necessary to attain equilibrium (next section).

Once this distribution is known, the slip amplitude and the displacement field generated over the free surface will be computed by superposition of the displacement fields due to each elementary dislocation. From the slip amplitude and the density change within the crack, $\Delta\rho = \rho_m - \rho_0$, the gravity anomaly can also be computed, assuming that the density of the host medium does not change appreciably. Displacement and gravity are the main observables that can be measured to test the model.

The main problem we face in the above scheme is assigning the equilibrium position of the crack tips, which define the integration domain of the integral equation, i.e. the depth up to which magma can rise for a given set of d , ρ_m , ρ_0 and p_0 . If an open conduit were available, the free surface of magma would reach a depth z_{\max} shallower than d , governed by the condition of hydrostatic equilibrium $p_0 - \rho_m g(d - z_{\max}) = 0$ (see Fig. 2). If such a conduit is not available, and we neglect crack-induced stresses, magma would reach a depth z_{eq} where its pressure equilibrates the lithostatic horizontal stress $p_0 - \rho_m g(d - z_{\text{eq}}) = \rho_0 g z_{\text{eq}} - \tau_0$ (with obvious modifications in the sedimentary case); the pressure within the crack would be greater than the pre-existing external pressure σ_0^L or σ_0^S over the whole depth range $d < z < z_{\text{eq}}$; this would give rise to a

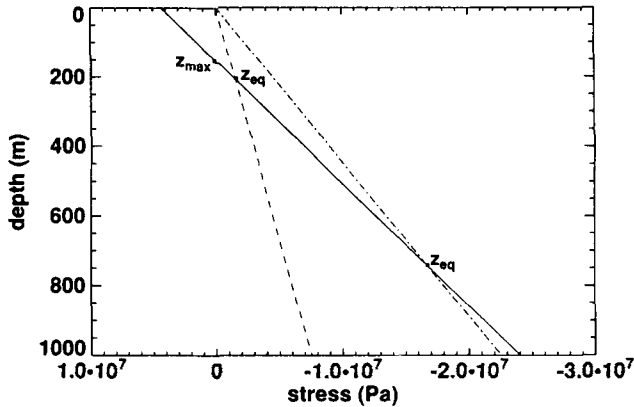


Figure 2. Initial state of stress σ_{xx} in the crust, as given by the lithostatic profile L (eq. 1a) dot-dashed, the sedimentary profile S (eq. 1b) dashed, and the hydrostatic profile in the magma (eq. 2) solid, for $d = 1000$ m, $p_0 = 2.4 \times 10^7$ Pa, $\rho_m = 2900$ kg m $^{-3}$, $\rho_0 = 2300$ kg m $^{-3}$, and $\tau_0 = 0$. The depths z_{eq} and z_{max} are indicated. The orientation of the stress axis is inverted to help interpretation in terms of pressure.

singular crack-induced stress σ_{xx}^c beyond the crack tip and to an ever-increasing stress intensity factor $K(p_0)$. We shall employ a different criterion: the equilibrium extension of the crack is not imposed *a priori*, but is found as part of the solution by imposing the constraint that the total stress component σ_{xx} (including the contributions σ^c generated by the crack itself) is non-tensional and finite beyond the crack tip. To this end we employ a variation of the technique originally proposed for shear cracks by Bonafede, Dragoni & Boschi (1985). We shall see that in this case the magma may rise above the depth z_{eq} , since the deformation produced by the emplacement of the dyke provides a suction (pressure drop) in the proximity of the crack tip. This criterion provides a final stress field which is continuous along the crack plane and can be made compatible with a pre-fractured (tensionally non-cohesive) medium. The relevance of such a model to volcanic situations is proved by the low magnitude (or even absence) of seismicity during some episodes of dyke emplacement (e.g. Rymer *et al.* 1994). We shall see also that the upper crack tip may be shallower than z_{max} for suitable values of p_0 , but that in such cases the magma must remain confined below the depth z_{max} , the rest of the crack being empty (or, more realistically, filled with gas). This feature was recognized by Barenblatt (1962) and Ali, Fehler & Das (1977) but has seldom been taken into account in previous models of dyke emplacement.

The reader who is not interested in the mathematical details of the solution may skip the following sections and go to the ‘results’.

MATHEMATICAL FORMULATION OF THE PROBLEM

We consider a layer of thickness d and density ρ_0 initially closed up by the lithostatic stress (1a). Magma then intrudes through a vertical crack, bringing the stress to the hydrostatic profile (eq. 2) over its plane. The difference $\sigma_m - \sigma_0^L$ has the role of ‘stress drop’ in shear cracks and shall be termed the ‘pressure rise’ in the following (since pressure has the opposite

sign to stress, the term ‘rise’ is employed as opposite to ‘drop’). It is this pressure difference that is responsible for the formation of a magma-filled crack: compression of the solid crust must take place in proximity to crack walls in order that the greater pressure imposed over the internal face by the fluid magma be balanced by normal tractions imposed over the external face by the solid crust.

From eqs (1a) and (2), the pressure that must be generated by compressional deformation on the external face of crack walls is

$$p(z) = -(\sigma_m - \sigma_0^L) = p_0 + \tau_0 - \rho_m g d + (\rho_m - \rho_0) g z, \quad d - \ell < z < d. \quad (3)$$

To simplify the solution, it is useful to consider a closed crack: as discussed in the previous section, we extend the pressure-rise profile (eq. 3) to $z > d$, symmetrically with respect to $z = d$. This choice, although arbitrary, is preferred to others (e.g. constant overpressure within the lower half-crack in the region $z > d$) because the overpressure in the source region, being due to differentiation processes, plausibly decreases with depth.

Let us introduce the non-dimensional coordinates

$$\zeta = \frac{z-d}{\ell}, \quad \xi = \frac{x}{\ell}, \quad \eta = \frac{y}{\ell}, \quad \delta = \frac{d}{\ell},$$

where ℓ is the crack half-length. Eq. (3) becomes

$$p(\zeta) = \Delta p_0 - (\rho_m - \rho_0) g \ell |\zeta|, \quad -1 < \zeta < 1, \quad (4)$$

where $\Delta p_0 = p_0 + \tau_0 - \rho_0 g d$ is the overpressure at $z = d$. Under this parametrization the upper crack tip is at $\zeta = -1$, its midpoint (where the magma pressure is p_0) is at $\zeta = 0$, its lower tip is at $\zeta = +1$.

The equilibrium crack equation for a distribution F of elementary tensile dislocations over a vertical plane is (from Ergodan *et al.* 1973)

$$\frac{\mu}{2\pi(1-\nu)} \mathcal{P} \int_b^c \frac{F(z')}{z' - z} dz' + \frac{1}{\pi} \int_b^c H(z, z') F(z') dz' = p(z), \quad b < z < c, \quad (5)$$

where \mathcal{P} denotes the ‘principal value’ of the integral that follows, b and $c = d \pm \ell$ are the positions of crack tips, and the kernel $H(z, z')$ is regular in $b < z' < c$:

$$H(z, z') = -\frac{1}{z' + z} + 6 \frac{z}{(z' + z)^2} - 4 \frac{z^2}{(z' + z)^3}. \quad (6)$$

It is probably useful to recall here the physical meaning of eq. (5): a tensile crack in a half-space, defined by the dislocation distribution F , produces over the crack plane $x = 0$ a stress contribution σ_{xx}^c given by the left-hand side of eq. (5); if F can be chosen so as to satisfy eq. (5) in $b < z < c$, the total pressure present over the crack domain $b < z < c$ is $-\sigma_m$, as given by the superposition of the initial pressure $-\sigma_0^L$ with the crack-induced pressure $-\sigma_{xx}^c = p$, with p given by eq. (3). Once F is known, the left-hand side of eq. (5) gives the crack-induced stress even when z lies outside the crack domain; in this case, since either $z < b$ or $z > c$, the singularity of the integrand disappears and the principal value in front of the former integral may be omitted.

METHOD OF SOLUTION

It is useful to expand the pressure-rise profile (eq. 4) in Chebyshev polynomials of the second kind, U_n , in the following way (e.g. Bonafede *et al.* 1985):

$$p(\zeta) = \frac{\mu}{1-\nu} \sum_{n=1}^{\infty} p_n U_{n-1}(\zeta),$$

where $p_n = \frac{2(1-\nu)}{\pi} \frac{1}{\mu} \int_{-1}^{+1} p(\zeta) U_{n-1}(\zeta) \sqrt{1-\zeta^2} d\zeta$, (7)

from which we obtain

$$p(\zeta) = \Delta p_0 - \frac{4(\rho_m - \rho_0)g\ell}{\pi} \times \sum_{n=0}^{+\infty} \frac{(-1)^{n+1}}{(2n+3)(2n-1)} U_{2n}(\zeta), \quad -1 < \zeta < +1. \quad (8)$$

Let us introduce in eqs (5) and (6) the non-dimensional coordinates ζ and $\zeta' = (z' - d)/\ell$, and define

$$\mathcal{F}(\zeta') = F(\zeta'\ell + d), \quad \mathcal{H}(\zeta, \zeta') = \ell H(\zeta\ell + d, \zeta'\ell + d). \quad (9)$$

Crack tips are at $\zeta = \pm 1$ and eq. (5) is rewritten as

$$\frac{1}{\pi} \frac{\mu}{2(1-\nu)} \left[\mathcal{P} \int_{-1}^{+1} \frac{\mathcal{F}(\zeta')}{\zeta' - \zeta} d\zeta' + \int_{-1}^{+1} \mathcal{H}(\zeta, \zeta') \mathcal{F}(\zeta') d\zeta' \right] = \Delta p_0 - \frac{4(\rho_m - \rho_0)g\ell}{\pi} \sum_{n=0}^{+\infty} \frac{(-1)^{n+1}}{(2n+3)(2n-1)} U_{2n}(\zeta). \quad (10)$$

Following Muskhelishvili (1953) we can split $\mathcal{F}(\zeta')$ into the product of a singular term $(1 - \zeta'^2)^{-1/2}$ times a regular function $g(\zeta')$ which can be expanded uniformly in Chebyshev polynomials of the first kind T_n :

$$\mathcal{F}(\zeta') = -\frac{1}{(1 - \zeta'^2)^{1/2}} \sum_{n=0}^{+\infty} \alpha_n T_n(\zeta'), \quad |\zeta'| < 1. \quad (11)$$

The 'closure condition' for the crack at $\zeta = \pm 1$ requires that the integral of \mathcal{F} over $(-1, 1)$ must vanish, i.e. that $\alpha_0 = 0$ (e.g. Bilby & Eshelby 1968). Inserting eq. (11) into eq. (10) we obtain

$$-\left(\frac{1}{2\pi}\right) \frac{\mu}{1-\nu} \sum_{n=1}^{+\infty} \alpha_n \left[\mathcal{P} \int_{-1}^{+1} \frac{T_n(\zeta')}{(\zeta' - \zeta)(1 - \zeta'^2)^{1/2}} d\zeta' + \int_{-1}^{+1} \mathcal{H}(\zeta, \zeta') \frac{T_n(\zeta')}{(1 - \zeta'^2)^{1/2}} d\zeta' \right] = \Delta p_0 - \frac{4(\rho_m - \rho_0)g\ell}{\pi} \times \sum_{n=0}^{+\infty} \frac{(-1)^{n+1}}{(2n+3)(2n-1)} U_{2n}(\zeta), \quad |\zeta| < 1. \quad (12)$$

The first integral above yields, for $|\zeta| < 1$, (e.g. Abramowitz & Stegun 1964)

$$\mathcal{P} \int_{-1}^{+1} \frac{T_n(\zeta')}{\zeta' - \zeta} \frac{d\zeta'}{\sqrt{1 - \zeta'^2}} = \begin{cases} \pi U_{n-1}(\zeta) & \text{if } n \geq 1 \\ 0 & \text{if } n = 0 \end{cases}. \quad (13)$$

Inserting eq. (6) into eq. (12), the second integral, which we

term $-\pi f_n(\zeta)$ for later convenience, becomes

$$-\pi f_n(\zeta) = \int_{-1}^{+1} \mathcal{H}(\zeta, \zeta') \frac{T_n(\zeta')}{(1 - \zeta'^2)^{1/2}} d\zeta' = - \int_{-1}^{+1} \frac{T_n(\zeta')}{(\zeta' + \zeta + 2\delta)(1 - \zeta'^2)^{1/2}} d\zeta' + 6(\zeta + \delta) \int_{-1}^{+1} \frac{T_n(\zeta')}{(\zeta' + \zeta + 2\delta)^2(1 - \zeta'^2)^{1/2}} d\zeta' - 4(\zeta + \delta)^2 \int_{-1}^{+1} \frac{T_n(\zeta')}{(\zeta' + \zeta + 2\delta)^3(1 - \zeta'^2)^{1/2}} d\zeta'. \quad (14)$$

Following Belardinelli & Bonafede (1991), this yields

$$f_n(\zeta) = \frac{(\zeta_3 - \zeta_2)^n}{\zeta_2} \left[1 - 6\zeta_1 \frac{n\zeta_3 + \zeta_2}{\zeta_3^2} + 2\zeta_1^2 \frac{(n^2 + 2)\zeta_3^2 + 3n\zeta_2\zeta_3 + 3}{\zeta_3^4} \right], \quad (15)$$

where $\zeta_1 = \zeta + \delta$, $\zeta_2 = \zeta + 2\delta$, $\zeta_3 = (\zeta_2^2 - 1)^{1/2}$ and $\delta = d/\ell$. Inserting this into eq. (12) we obtain

$$\frac{1}{2} \frac{\mu}{(1-\nu)} \sum_{n=1}^{+\infty} \alpha_n [U_{n-1}(\zeta) - f_n(\zeta)] = -\Delta p_0 + \frac{4(\rho_m - \rho_0)\rho g\ell}{\pi} \sum_{n=0}^{+\infty} \frac{(-1)^{n+1}}{(2n+3)(2n-1)} U_{2n}(\zeta). \quad (16)$$

Chebyshev polynomials of the second kind are a complete set of orthogonal functions over the interval $(-1, 1)$ if the measure $(1 - \zeta^2)^{1/2} d\zeta$ is employed. Therefore, multiplying eq. (16) by $(1 - \zeta^2)^{1/2} U_{k-1}(\zeta)$ and integrating over $(-1, 1)$, we obtain

$$\frac{1}{2} \frac{\mu}{(1-\nu)} \left[\alpha_k - \sum_{n=1}^{+\infty} \Gamma_{k,n}(\delta) \alpha_n \right] = -\Delta p_0 \delta_{1,k} + 4 \frac{(\rho_m - \rho_0)g\ell}{\pi} \times \begin{cases} 0, & \text{if } k \text{ is even,} \\ \frac{(-1)^{(k+1)/2}}{k^2 - 4}, & \text{if } k \text{ is odd,} \end{cases} \quad (17)$$

where $\delta = d/\ell$ and δ_{ij} is the Kronecker delta. The matrix elements $\Gamma_{k,n}(\delta)$ are

$$\Gamma_{k,n}(\delta) = \frac{2}{\pi} \int_{-1}^{+1} \sqrt{1 - \zeta^2} U_{k-1}(\zeta) f_n(\zeta) d\zeta. \quad (18)$$

The integrals (18) have no analytic expression for arbitrary values of k and n ; they were computed numerically employing Gaussian quadrature formulas. Furthermore, the system (17) for α_n is infinite and will be solved numerically after truncation to a suitable finite order N . As to the truncation order, typically we keep it above 100, even if much smaller truncations generally give good results, apart from sharp features.

Representing the α_n coefficients as a vector, eq. (17) becomes

$$(\mathbf{I} - \mathbf{\Gamma})\boldsymbol{\alpha} = \boldsymbol{\beta}, \quad (19)$$

where \mathbf{I} is the identity matrix, even components of $\boldsymbol{\beta}$ vanish and odd components are given by

$$\beta_k = \frac{2(1-\nu)}{\mu} \left[-\Delta p_0 \delta_{1,k} + \frac{4(\rho_m - \rho_0)g\ell}{\pi} \frac{(-1)^{(k+1)/2}}{k^2 - 4} \right], \quad k \text{ odd.} \quad (20)$$

The matrix $\mathbf{I} - \mathbf{\Gamma}$ is then inverted numerically to retrieve the coefficients α_n :

$$\alpha = (\mathbf{I} - \mathbf{\Gamma})^{-1} \beta \tag{21}$$

In solving eq. (21), all parameters (p_0, ρ_m, ρ_0, d and ℓ) must be specified. Accordingly, α is a function of these. In order to impose the non-singularity condition at the upper crack tip ($\zeta = -1$), p_0, ρ_m, ρ_0 and d are fixed and the extra condition is imposed (Bonafede *et al.* 1985) that

$$\sum_{n=1}^N (-1)^n \alpha_n(\ell) = 0. \tag{22}$$

This condition, which describes the arrest configuration of a crack under a stress threshold criterion, makes the residual stress field finite and continuous at the upper crack tip. The extra condition (22) can only be satisfied if the initial stress field is suitably non-uniform (i.e. if negative pressure-rise regions exist over the crack plane) and ℓ is chosen appropriately. Accordingly, we employ (22) as an implicit equation for ℓ to be solved numerically. We do not impose the non-singularity condition at the lower tip $\zeta = +1$, since the details of the crack there have no practical effect on near-surface quantities. In other terms, the position of the lower tip is imposed at $z = d + \ell$. It should be noted that, even if the 'pressure-rise' is continued symmetrically beyond depth d , the problem is non-symmetric because of the presence of the free surface at $z = 0$, which is accounted for by the matrix $\mathbf{\Gamma}$.

It is interesting to study what happens in the region between the crack tip and the free surface, i.e. for $-\delta < \zeta < -1$. As noted after eq. (5), once the α_n coefficients are known, the crack-induced stress component σ_{xx}^c over the crack plane may be computed as the left-hand side of (12) for $\zeta < -1$:

$$\sigma_{xx}^c(\zeta) = -\frac{\mu}{2(1-\nu)} \sum_{n=1}^{+\infty} \alpha_n \left[\frac{(\zeta + \sqrt{\zeta^2 - 1})^n}{\sqrt{\zeta^2 - 1}} - f_n(\zeta) \right], \tag{23}$$

$-\delta < \zeta < -1.$

In order to obtain the total stress σ_{xx} , the initial stress (1a) must be added to eq. (23).

Finally, by integrating eq. (11) from -1 to ζ , we can find the slip function Δu , expanded in Chebyshev polynomials:

$$\Delta u(\zeta) = \ell \sqrt{1 - \zeta^2} \sum_{n=1}^{+\infty} \frac{\alpha_n}{n} U_{n-1}(\zeta). \tag{24}$$

The displacement field produced by the crack over the free surface is one of the most important observables. The vertical displacement at $z = 0$, due to an elementary tensile dislocation at $z = z'$ with Burger's vector $\mathbf{B} = B\mathbf{i}$, is

$$w_e(x) = -\frac{B}{\pi} \frac{x^2}{(z'^2 + x^2)}. \tag{25}$$

This expression may be obtained either from actual solution of the tensile dislocation problem in a half-space (Danesi 1994), or from Davis (1983), who gives the displacement due to a rectangular dislocation surface, after taking the appropriate limits.

For the variable-slip crack given by eq. (24), the vertical displacement due to elastic deformation is obtained by integration of (25) over the crack plane, with B replaced by the

dislocation density (11):

$$W(\xi) = -\frac{\ell \xi^2}{\pi} \sum_{n=1}^{+\infty} \alpha_n \int_{-1}^1 \frac{T_n(\zeta')}{\sqrt{1 - \zeta'^2} [\xi^2 + (\delta + \zeta')^2]} d\zeta', \tag{26}$$

where $\xi = x/\ell$.

It should be noted that, since any crack model can be built from weighted superposition of elementary dislocations (e.g. Landau & Lifchitz 1967), from eq. (25) vanishing vertical displacements are obtained at $x = 0$ for any vertical-crack model in a homogeneous half-space.

The density difference between magma and host rock, and the compression within the rock generated by the crack opening also provide a vertical body force directed downwards, which can be computed from Mindlin's (1936) Green's function solution; details are not shown here, but this gravity contribution to surface displacement can be shown to be generally negligible (of the order of 1 cm).

THE GRAVITY ANOMALY

Another important observable related to dyke intrusion is the gravity anomaly measured at the ground surface. The gravity change at a point $(x, y, 0)$ of the ground surface, due to a small volume dV' around the point $(0, y', z')$, where a density anomaly $\Delta\rho$ is present, can be computed from

$$dg = \frac{G\Delta\rho dV'}{x^2 + (y - y')^2 + z'^2} \cos \alpha, \tag{27}$$

with $\cos \alpha = \frac{z'}{\sqrt{x^2 + (y - y')^2 + z'^2}},$

where $G = 6.67 \times 10^{-11} \text{ N m}^2 \text{ kg}^{-2}$ is the gravitational constant.

The volume element dV' over which the density anomaly is present can be written as $dy' dz' \Delta u(z')$. Integrating eq. (27) over the crack plane, we find the total gravity anomaly on the free surface $\Delta g(x)$:

$$\Delta g = G \int_{-\infty}^{+\infty} dy' \int_{d-\ell}^d dz' \frac{z' \Delta\rho(z') \Delta u(z')}{[x^2 + (y - y')^2 + z'^2]^{3/2}}. \tag{28}$$

Introducing the usual dimensionless variables $\zeta' = (z' - d)/\ell$, $\eta = y/\ell$, $\eta' = y'/\ell$, $\xi = x/\ell$ and substituting $\Delta u(\zeta')$ from eq. (24), the integration over $d\eta'$ can be performed, yielding

$$\Delta g(\xi) = 2G\ell \sum_{n=1}^{+\infty} \frac{\alpha_n}{n} \int_{-1}^0 \Delta\rho(\zeta') \times \frac{\delta + \zeta'}{\xi^2 + (\delta + \zeta')^2} U_{n-1}(\zeta') \sqrt{1 - \zeta'^2} d\zeta'. \tag{29}$$

Of course, this result is independent of η or y , because our crack model is assumed to be in a plane-strain configuration. Setting $\zeta' = \cos \theta$, we have

$$\Delta g(\xi) = 2G\ell \sum_{n=1}^{+\infty} \frac{\alpha_n}{n} \int_{\pi/2}^{\pi} \Delta\rho(\cos \theta) \times \frac{\delta + \cos \theta}{\xi^2 + (\delta + \cos \theta)^2} \sin n\theta \sin \theta d\theta. \tag{30}$$

If the dyke is completely filled with magma, $\Delta\rho = \rho_m - \rho_0$; however, we shall see that in some cases a portion of the crack remains empty of magma and $\Delta\rho = -\rho_0$ there. Note that a further contribution to the gravity field comes from the density

change in the host rock due to the contraction/dilatation of the medium surrounding the crack. This contribution is not modelled in the present paper.

RESULTS

We have derived in the previous sections formulae to compute the stress field, the crack slip and extension over the crack plane, the vertical displacement and the gravity anomaly on the free surface of a cohesionless medium, for a given set of fixed parameters: the pressure p_0 at the bottom of the layer, the rock and magma densities ρ_0 and ρ_m , the layer thickness d , its rigidity μ and Poisson ratio ν . For the sake of simplicity, the tectonic stress contribution τ_0 in eq. (1) is ignored.

Typical values for shallow volcano-sedimentary layers are $\mu = 3 \times 10^9$ Pa, $\nu = 0.25$, and $\rho_0 = 2300$ kg m⁻³; several cases are considered for the remaining parameters: lithostatic (L) and sedimentary (S) initial states are assumed, as given by eqs (1a) and (1b); small ($d = 1$ km) and large ($d = 3$ km) depth values have been employed, marked with digits '1' and '3', respectively; high ($\rho_m = 2900$ kg m⁻³) and low ($\rho_m = 2600$ kg m⁻³) magma densities are considered, marked as '+' and '-', respectively. Accordingly, model [L1+] assumes: lithostatic initial state, $d = 1$ km and $\rho_m = 2900$ kg m⁻³, model [S1+] assumes sedimentary equilibrium and so on.

For each of the previous models, the problem has been solved for a set of values of the pressure p_0 , ranging from a lower bound corresponding to negative pressure rise everywhere over $0 < z < d$, to an upper bound corresponding to positive pressure rise over the same domain.

In Fig. 3 the total stress component σ_{xx} is plotted over the crack plane for model [L1+]. The position of the crack tip can be inferred from the cusp in the stress profile. We can appreciate that no singularity is present at the crack tip $b =$

$d - \ell$, and that the total stress field is continuous there. Crack contributions can be better appreciated in Fig. 4(a), where the lithostatic profile (eq. 1a) is subtracted from σ_{xx} . All profiles, computed for increasing values of p_0 , conform to the hydrostatic magma profile σ_m (see eq. 2) from $z = b = d - \ell$ to $z = d$, and decrease sharply above the crack tip. All profiles provide negative (i.e. compressive) total stress, apart from the dashed profile, which is accordingly unacceptable for a medium with vanishing tensional strength. We can understand easily what happens as p_0 is increased: the crack provides a compressive contribution to the stress field over the depth range $z_{eq} < z < d$, but it provides a tensile contribution over $z_{eq} < z < 0$ (z_{eq} is the depth where magma pressure is equal to the lithostatic pressure). As far as this tensile contribution does not exceed the lithostatic pressure at the crack tip, the total stress is compressive and the medium behaves elastically (thin solid lines in Figs 3 and 4). As p_0 increases, the crack tip migrates towards the free surface, the lithostatic pressure at the tip becomes smaller and the tensile stress contribution is higher, because the crack length increases and the distance from the free surface decreases. Eventually, the total stress becomes positive at the crack tip, and all the way to the surface (e.g. the dashed lines in Figs 3 and 4): in this situation, since the medium is assumed to be tensionally non-cohesive, the fracture must reach the surface while magma remains confined below the depth z_{max} ; as long as $p_0 < \rho_m g d$ the dyke is non-eruptive.

The crack width or slip profile $\Delta u(z)$ is plotted in Fig. 4(b). $\Delta u(z)$ vanishes with zero derivative at the crack tip, whilst singular crack models would provide an infinite derivative there; this feature is strictly related to the non-singularity condition (22). It must be stressed, however, that the crack width is very small (less than 1 m) under the assumption of lithostatic equilibrium: under these circumstances, the time needed for solidification of magma within the dyke would be

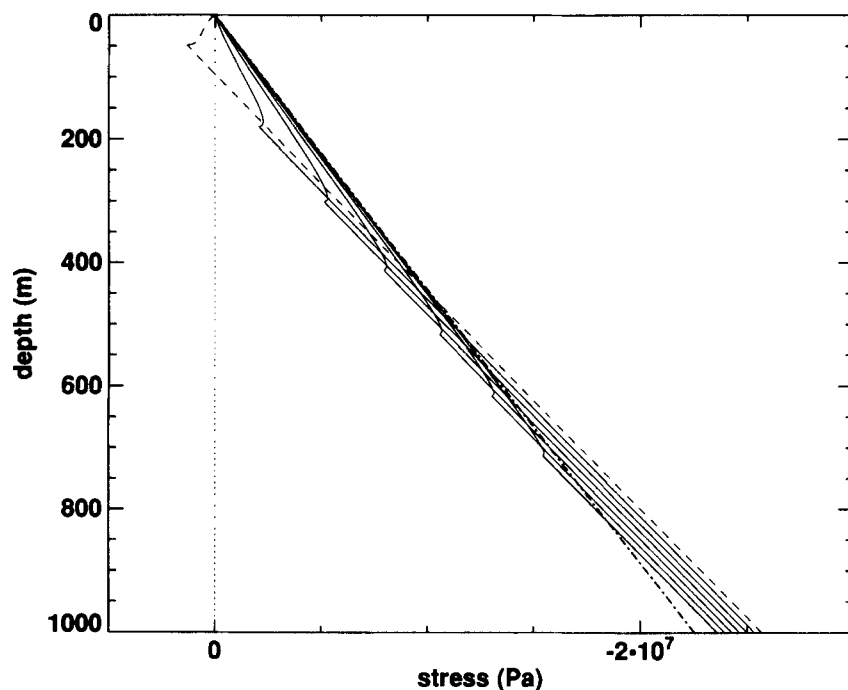


Figure 3. Total stress profiles σ_{xx} ($x = 0, z$) over the crack plane (solid lines), for model [L1+] and a set of values for p_0 between 2.3×10^7 and 2.6×10^7 Pa. The vertical dotted line is the zero total-stress line, the dot-dashed line is the lithostatic profile, and the dashed line is a total stress profile that would yield tensional total stress in $0 < z < d - \ell$ and negative pressure in the magma; it is therefore unacceptable.

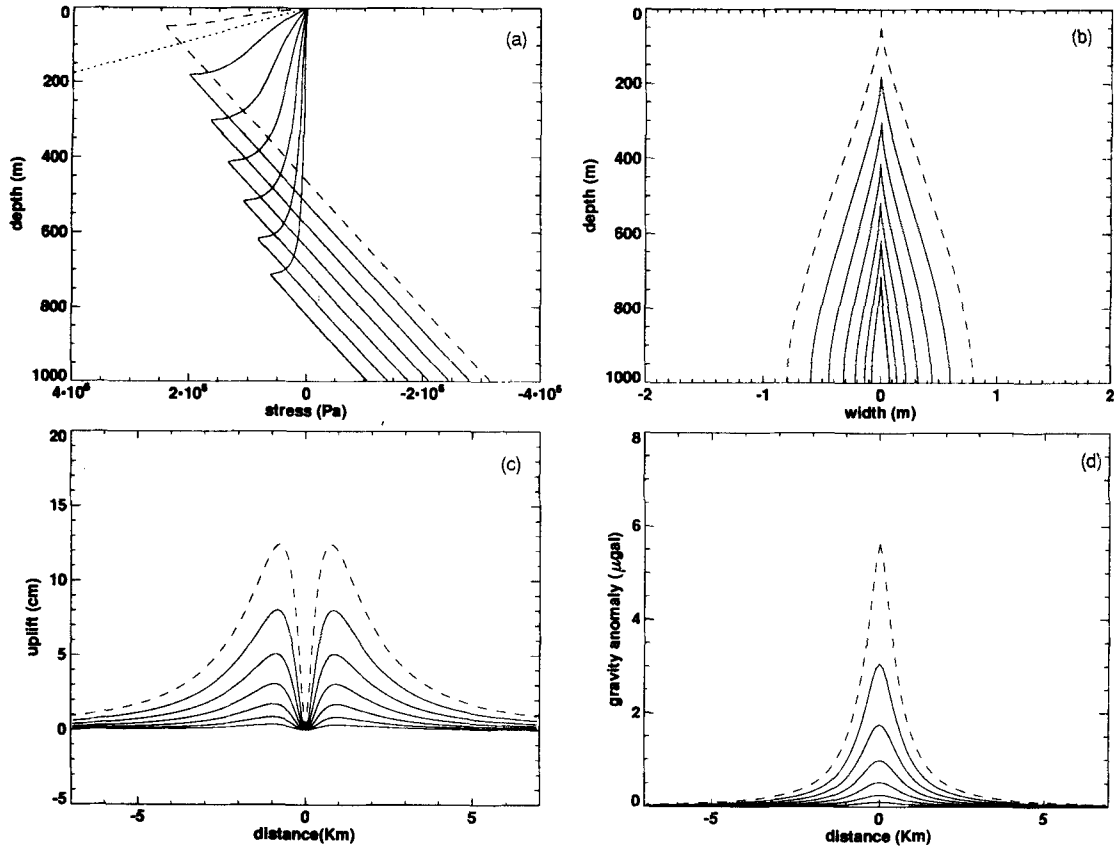


Figure 4. Crack-induced stress component σ_{xx}^c (panel a), slip function Δu (b), vertical component of surface displacement $W(x)$ (c) and surface gravity anomaly (d) for model [L1+] and values of p_0 as in Fig. 3. The dotted line in panel (a) reproduces the zero total-stress line of Fig. 3; the dashed profiles are unacceptable.

less than 3 days (e.g. Turcotte & Schubert 1982). Where the pressure rise is positive (i.e. from $z = z_{eq}$ to $z = d$), the crack is concave inwards, and where the pressure rise is negative (from the crack tip $z = d - \ell$ to $z = z_{eq}$), it is concave outwards. The implications of this ‘suction’ region, which develops around the upper portion of the crack, are discussed in the next section.

The vertical displacement $W(x)$ on the free surface, computed from eq. (26), is plotted in Fig. 4(c). The shape is similar to those provided by Pollard *et al.* (1983) for an elliptical crack, and by Davis (1985) for a rectangular crack. Even in this case, however, the amount of displacement is rather small, compared with several observations.

Finally, the gravity anomaly is computed from eq. (30) and plotted in Fig. 4(d). The anomaly is very narrow but, again, it is very small if compared with measurements recently carried out over Mount Etna; computed values are typically less than $5 \mu\text{gal}$ above the crack, while measured peak values (after removing contributions ascribed to uplift) are $20 \mu\text{gal}$ (Budetta *et al.* 1989) and $100 \mu\text{gal}$ (Rymer *et al.* 1993). Indeed, Rymer *et al.* (1993) speculate that such a big anomaly would require magma emplacement within a previously empty cavity 4 m wide and 1 km deep. It therefore seems necessary to change the model parameters in order to increase Δu .

One possibility of obtaining a larger Δu is to increase the pressure rise, other things being equal. This cannot be accomplished in a cohesionless medium with a lithostatic initial profile since tensional stresses are obtained if p_0 is increased further (the dashed lines in Fig. 4), but it can be

done in the [S1+] model, where a sedimentary initial stress state is assumed.

The solution technique is the same as in the lithostatic case, apart from the ‘pressure-rise’ profile (eq. 3), which is now substituted by

$$p(z) = -(\sigma_m - \sigma_0^s) = p_0 + \tau_0 - \rho_m g d + \left(\rho_m - \frac{\nu}{1 - \nu} \rho_0 \right) g z. \quad (31)$$

This simply amounts to replacing ρ_0 in eq. (3) with the effective density $\rho'_0 = (\nu/1 - \nu)\rho_0$. The pressure p_0 necessary to open the crack is smaller than in the lithostatic case. Of course, the real density difference $\rho_m - \rho_0$ must still appear in the equation for the gravity anomaly (eq. 29).

Results are shown in Figs 5 and 6. In this case, the dyke is still confined to great depth when a tensile total stress develops (dashed lines) in the proximity of the upper tip. The crack in model [S1+] is wider than in [L1+], but the vertical displacement and the gravity anomaly are still too small compared with the observations mentioned, due to the greater distance from the surface.

However, in the dashed profiles of model [S1+] the total stress above the crack tip reverts to negative values going towards the surface; hence, the crack will not open to the surface as in model [L1+]. Can the crack tip be shallower than z_{max} ? What should be the crack configuration if this happens? Even if we were to allow positive stress values in the

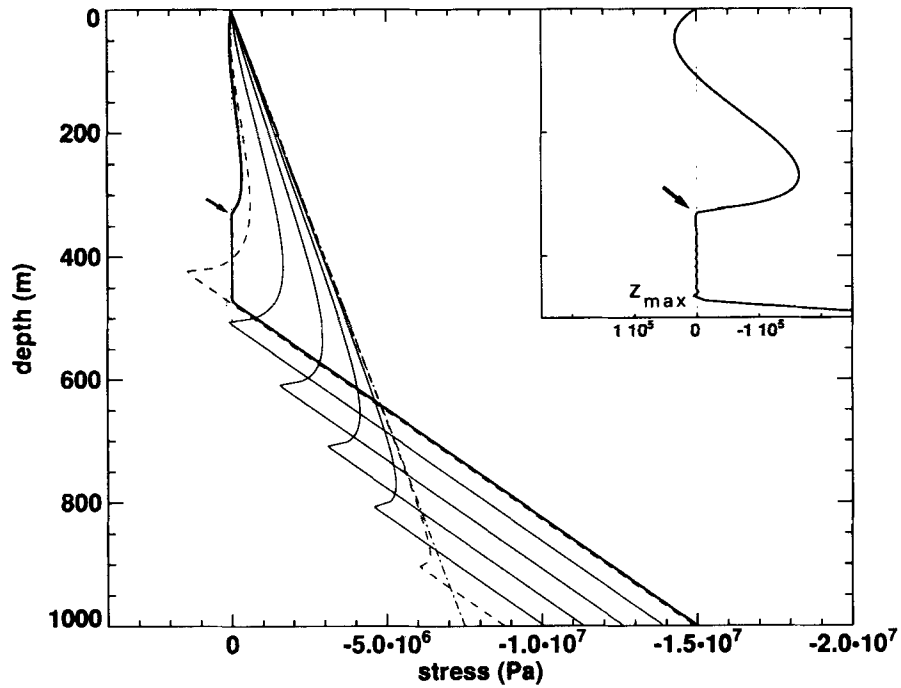


Figure 5. As Fig. 3, but for a sedimentary initial-stress profile (model [S1+]) and values of p_0 between 9 and 15 MPa. The dashed profile is unacceptable. The thick solid profile is acceptable and provides a void open crack between the crack tip (indicated by an arrow) and the depth z_{max} (the inset shows the total stress in the uppermost region, magnified 10 times).

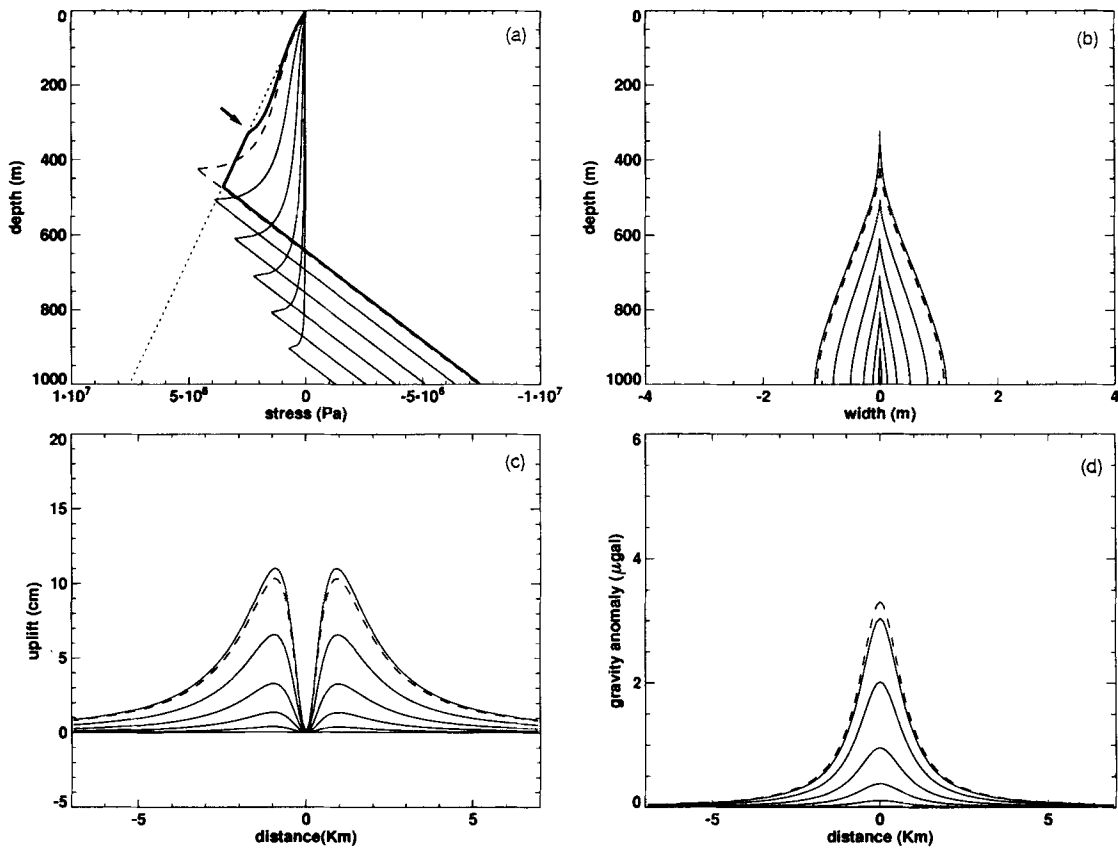


Figure 6. As Fig. 4, but for a sedimentary initial-stress profile (model [S1+]). The uppermost solid profiles correspond to the partially void crack with upper tip shallower than z_{max} .

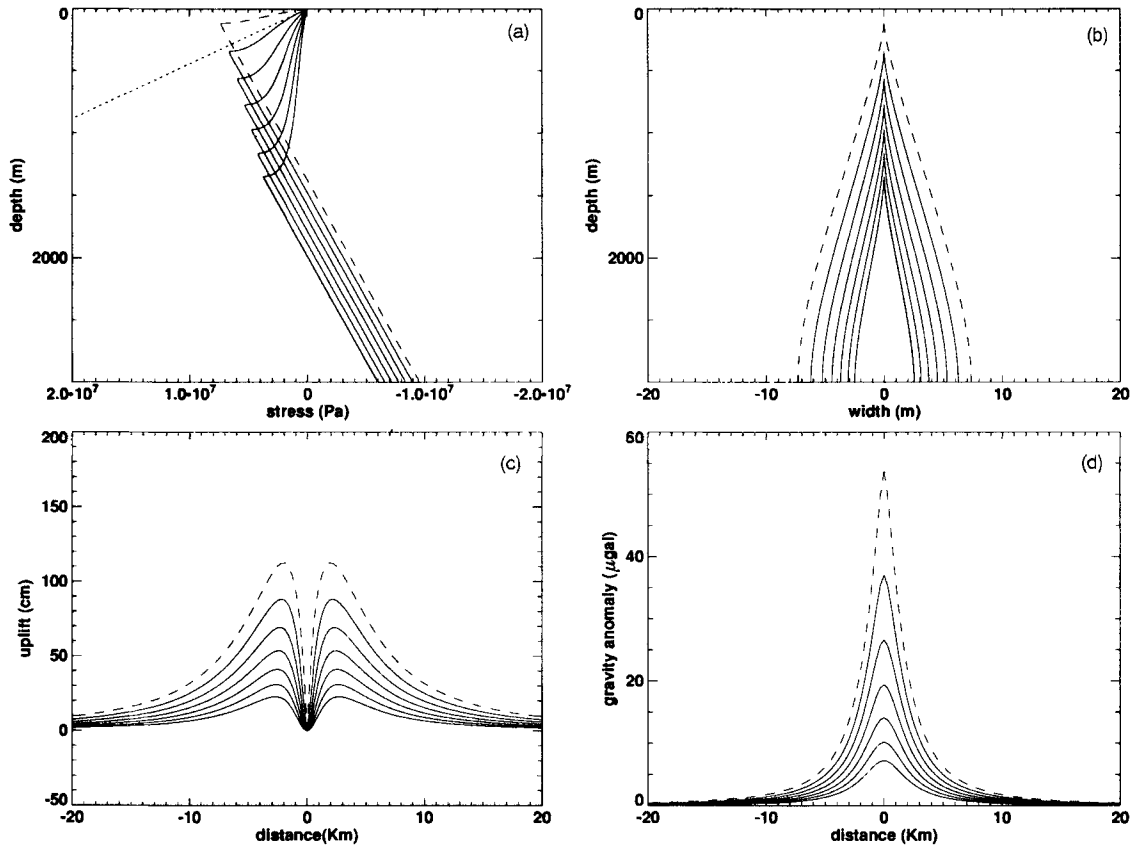


Figure 7. As Fig. 4, for $d = 3$ km (model [L3+]).

solid medium (thus dismissing the cohesionless assumption), the portion of the crack above z_{\max} cannot be filled with magma since the hydrostatic gradient would bring the absolute pressure to negative values (dashed line in Fig. 5), and a negative pressure is meaningless. The upper portion of the crack (above z_{\max}) must be empty (or filled with gas), in the same way as the upper part of the glass tube in a mercury barometer remains empty. Accordingly, the absolute pressure within the crack subdomain $z < z_{\max}$ must vanish (neglecting gas pressure). This requires an obvious modification to eq. (2) to provide vanishing pressure values when $z < z_{\max}$. The resulting configuration is shown by the thick line in Fig. 5. In this configuration, of course, the density anomaly $\Delta\rho$, is employed in computing the gravity change in eq. (28), is $\rho_m - \rho_0$ only if $d < z < z_{\max}$, but it is $-\rho_0$ if $z_{\max} < z < d - \ell$. The results shown in Figs 5 and 6 show that the total stress is negative (i.e. compressive) above the crack tip, but that it becomes positive again in the proximity of the free surface. Accordingly, in a cohesionless medium, open fissures must develop over the ground surface, which are mechanically related but not connected with the dyke. With this extension of model [S1+], the crack tip can be very shallow; however, the vertical displacement and the gravity anomaly (Fig. 6) are still too low with respect to several observations, due to the extreme narrowing of the crack width in the proximity of the tip.

Another way of increasing the values of ground deformation and gravity anomaly is to increase the vertical extension of the dyke. Fig. 7 shows the results for model [L3+]. In this case the crack width can be greater than 15 m, and the uplift

and gravity anomaly can reach values comparable with observations on Mt Etna. Figs 8 and 9 show results for model [S3+]: compared with model [L3+], lower values are obtained for both the uplift and the gravity anomaly, as long as the crack tip is confined at deeper than z_{\max} . However, if the configuration with crack tip shallower than z_{\max} (thick line in Fig. 8) is computed, according to the considerations already made for model [S1+], we see that the computed vertical displacement and gravity anomaly become comparable to some observations (uppermost solid lines in Fig. 9).

In Figs 10 and 11, results are shown for models [L3-] and [S3-], in which the magma density is taken as 2600 kg m^{-3} , the uplift can be as high as 50 cm but the gravity anomaly is less than $10 \mu\text{gal}$.

DISCUSSION AND CONCLUSIONS

Gravity anomalies and vertical surface displacements related to dyke intrusion are two independent constraints on their common source. Any physically sound model of dyke injection should be able to reproduce both observations simultaneously. In a crack model, the pressure-rise profile within the dyke is the main factor responsible for both, since it governs the opening width of the crack and this in turn determines the deformation field and the mass input. If the host rock is assumed to be cohesionless, i.e. it is unable to sustain tensional tractions, the vertical extension of the crack can be also computed from the pressure rise and the problem is completely specified once the initial state of stress, the depth of dyke injection and the densities of rock and magma are given.

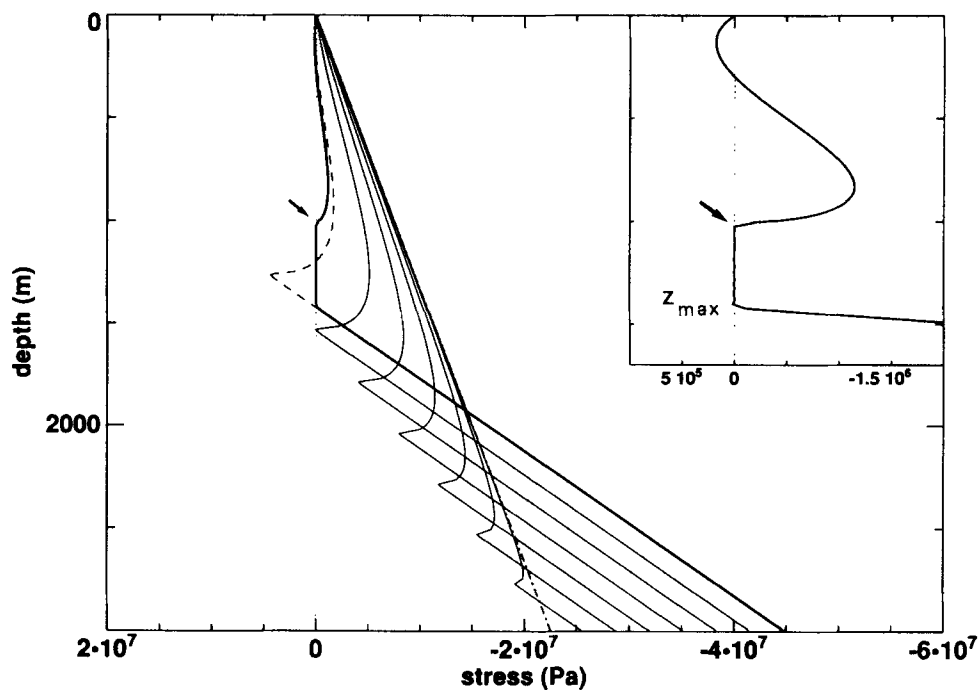


Figure 8. Total-stress profiles σ_{xx} ($x=0, z$) over the crack plane (solid lines), for model [S3+] and a set of values for p_0 between 2.5×10^7 and 4.5×10^7 Pa. The vertical dotted line is the zero total-stress line, and the dot-dashed line is the initial sedimentary profile; the dashed line is unacceptable. The thick solid profile is acceptable and provides a void open crack between the crack tip (indicated by an arrow) and the depth z_{\max} (the inset shows the total stress in the uppermost region, magnified 10 times).

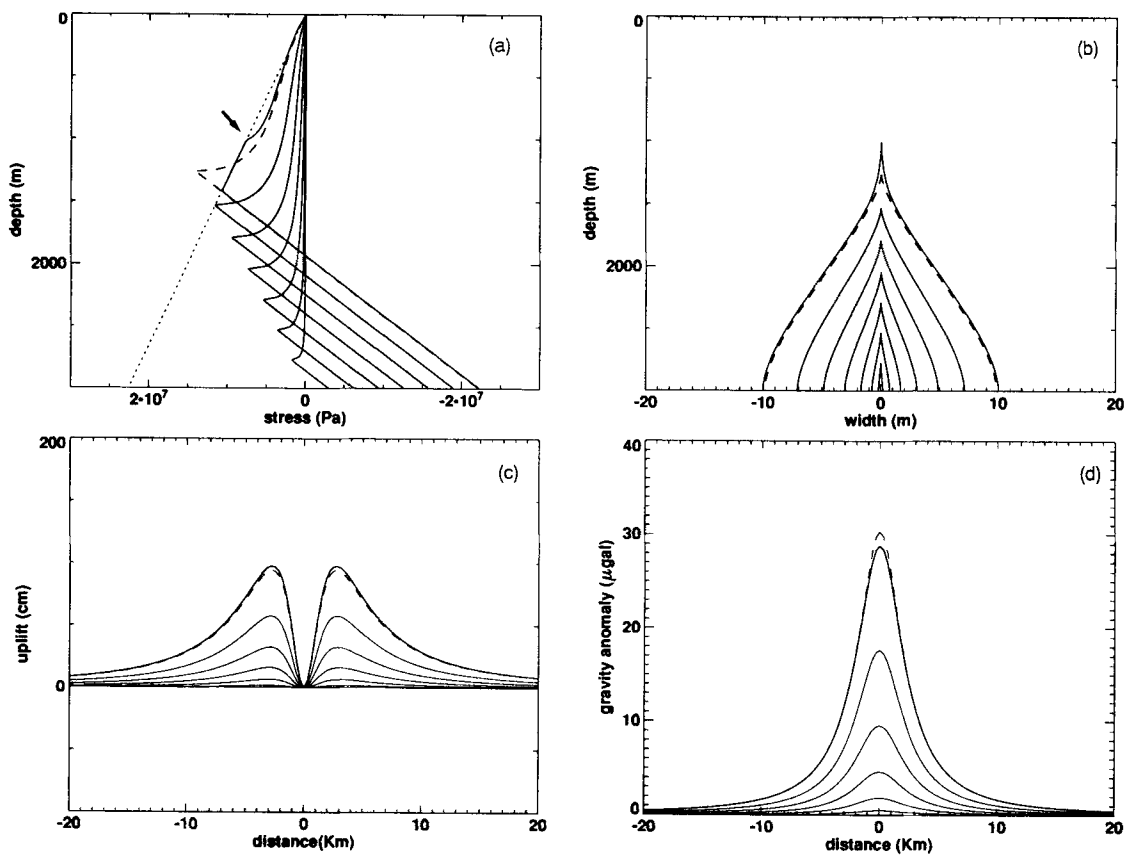


Figure 9. As Fig. 4, for model [S3+]. Profiles computed for crack tips shallower than z_{\max} are shown (uppermost solid lines).

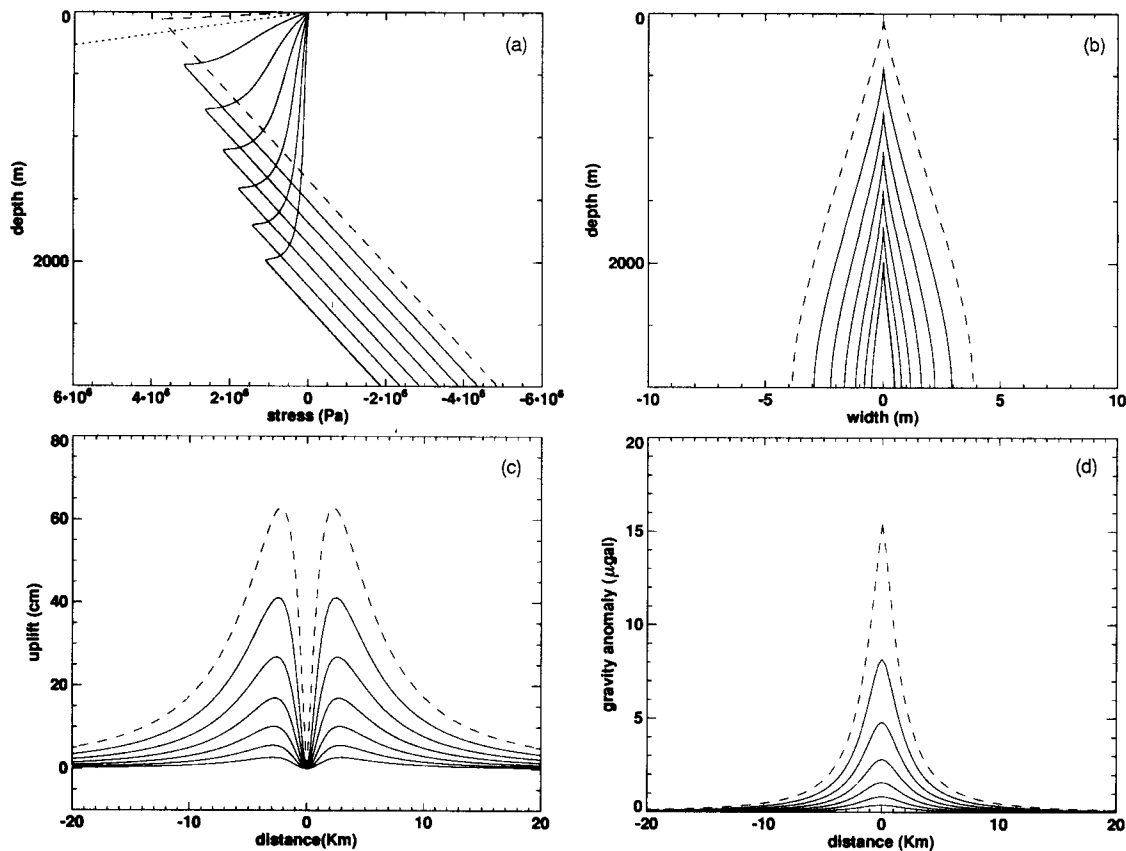


Figure 10. As Fig. 4, for $d = 3$ km and $\rho_m = 2600$ kg m $^{-3}$ (model [L3-]).

In model [L1+] the initial stress is lithostatic, the depth of injection is 1 km and the density difference is 600 kg m $^{-3}$. In this case the opening width of the crack is too small to reproduce the displacement field and the gravity anomaly observed on Mt Etna by Murray (1994) and Rymer *et al.* (1993). We then considered other possibilities, such as a sedimentary initial state (model [S1+]) and a deeper injection level (models [L3+], [S3+]), which yield larger values for the crack width, uplift and gravity changes. The main result is that uplift values comparable to observations (up to 1 m) can be obtained, while gravity changes as large as 100 μ gal are difficult to reproduce. However, in the computation of gravity anomalies we have neglected the density changes within the host rock, which are due to the non-vanishing trace of the strain tensor induced by crack opening. We assumed that this contribution was negligible, since rocks are nearly incompressible, but this is strictly the case only if $\nu = 1/2$. The unsatisfactory results obtained in modelling large gravity changes compel one to reconsider this assumption according to the following gross argument: if the host rock displacement caused by dyke injection were to vanish within a negligibly short distance from the crack plane, the excess mass responsible for the gravity change would be $\rho_m dV'$ instead of $\Delta\rho dV'$ in eq. (27), and the gravity changes shown in Figs 4–9 should be multiplied by a factor $\rho_m/(\rho_m - \rho_0) \sim 4.8$, and those in Figs 10 and 11 by a factor ~ 8.7 . Of course a correct computation of the gravity change must take into account the fact that not only compressions but also dilatations are present in the medium and

that rock deformation is expected to be spread laterally over a large region, comparable to crack length.

If we dismiss the assumption of negligible tensile strength, and allow infinite stress at the crack tip, as is the case for classical crack models with constant, positive pressure rise Δp_0 , we might increase Δp_0 above the hydrostatic limit $(\rho_m - \rho_0)gd$ without giving rise to an eruption, since in such a case the crack length ℓ is no longer controlled by the pressure rise alone, the condition for crack propagation being determined by the stress intensity factor K becoming greater than a critical value K_c . Such a model, in which the medium is assumed to possess a significant tensile strength, might be suitable to describe dyke injection up to a depth where it meets a competent layer. Since, however, K is an increasing function of both ℓ and Δp_0 , once the critical value for propagation is achieved, we should expect a large shallow earthquake followed by catastrophic crack propagation to the surface.

On the other hand, the solutions for a cohesionless medium provide results which can be important in several respects in understanding observations related to dyke intrusion. For instance, the 7 km long, non-eruptive fracture observed on the south flank of Mount Etna during the 1989 eruption (which took place on the eastern flank) may be explained in terms of an elongated fissure system related but not connected to a buried dyke. The lack of significant seismic activity (at least in the first days) is an indication of little cohesion of the host rock, while the lack of any visible degassing activity along this fracture may also be explained in terms of (i) the lack of any

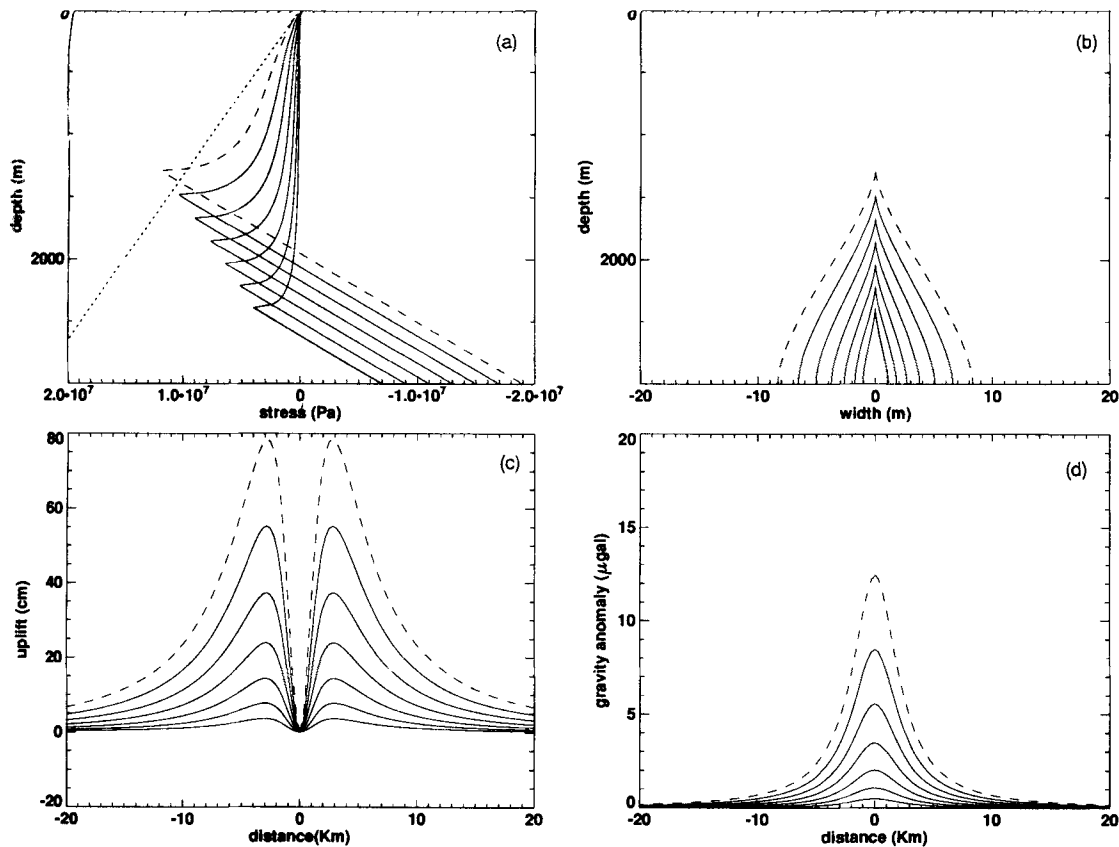


Figure 11. As Fig. 4, but for a sedimentary initial stress profile, $d = 3$ km and $\rho_m = 2600 \text{ kg m}^{-3}$ (model [S3–]).

connection between the magma-filled dyke and surface fissures discussed in connection with Figs 5 and 6, and (ii) the suction (pressure drop) provided by the present model in the proximity of the crack tip (i.e. over $0 \leq z \leq z_{eq}$, Fig. 2), which drives an inflow of fluids from the surrounding regions.

Another important role that can be played by the suction region is when a high-permeability aquifer is present along the dyke path; in such a case, hydro-magmatic interaction would be possible since the water would be at a higher pressure (possibly, the lithostatic value) than the magma over all the depth range $0 < z < z_{eq}$ and in particular over the crack domain from the tip depth $d - \ell$ to z_{eq} . In singular crack models with positive pressure rise, the inflow condition is attained only above the crack tip, never adjacent to the magma-filled domain.

Finally, several of the points considered above need to be discussed and investigated with greater care in future work. We have already said this about the gravity change, and the need to compute in a rigorous way the density change in the host rock. Another limitation of the present model is its static approach; the hydrostatic stress profiles for magma within the dyke are realistic only if magma is still. Speaking of dyke propagation as we did in the previous sections is therefore appropriate only for slow propagation, since otherwise a pressure gradient in excess of the hydrostatic value should be taken into account to overcome the viscous drag at crack walls, and the variable crack section would significantly affect the flow itself (see, e.g., Spence & Turcotte 1985). Furthermore, magma density has been taken as uniform at every depth, while its ascent towards the surface is generally accompanied by a density decrease (e.g. Kushiro 1980) related to fraction-

ation, differentiation and release of volatiles producing gas bubbles. Finally, thermally activated processes (e.g. viscoelasticity) in the host rock surrounding the magma-filled crack should be taken into account and might help in explaining the time lag between gravity changes and ground displacement (Rymer *et al.* 1994).

These problems will possibly be addressed in future papers.

ACKNOWLEDGMENTS

Comments by two anonymous referees were very helpful in preparing the present revision and correcting an arithmetic blunder in the original version. The work was carried out with financial contributions from GNV and MURST.

REFERENCES

- Abramovitz, M. & Stegun, I.A., 1964. *Handbook of mathematical functions*, Dover, Washington, DC.
- Aki, K., Fehler, M. & Das, S., 1977. Source mechanism of volcanic tremor: fluid driven crack models and their application to the 1963 Kilauea eruption, *J. Volc. Geotherm. Res.*, **2**, 259–287.
- Barenblatt, G.I., 1962. The mathematical theory of equilibrium cracks in brittle fracture, *Adv. appl. Mech.*, **7**, 55–129.
- Belardinelli, M.E. & Bonafede, M., 1991. A crack model of afterslip on shallow faults, *Geophys. J. Int.*, **106**, 521–530.
- Bilby, B.A. & Eshelby, J.D., 1968. Dislocations and the theory of fracture, in *Fracture—an Advanced Treatise*, Vol. I, pp. 99–182, ed. Liebowitz, H., Academic Press, New York.
- Bonafede, M., 1990. Axi-symmetric deformation of a thermo-poro-

- elastic half-space: inflation of a magma chamber, *Geophys. J. Int.*, **103**, 289–299.
- Bonafede, M., Dragoni, M. & Boschi, E., 1985. Quasi-static crack models and the frictional stress threshold criterion for slip arrest, *Geophys. J. R. astr. Soc.*, **83**, 615–637.
- Budetta, G., Grimaldi, M. & Luongo, G., 1989. Variazioni temporali di gravità nell'area etnea (1986–1989), *Bollettino del Gruppo Nazionale Vulcanologia*, **1**, 137–146 (in Italian).
- Budetta, G., Grimaldi, M. & Luongo, G., 1990. Gravity variations, in *Mt Etna: the 1989 eruption*, pp. 56–57, eds Barberi, F., Bertagnini, A. & Landi, P., C.N.R., Gruppo Nazionale Vulcanologia, Giardini, Pisa.
- Danesi, S., 1994. Deformazione sulla superficie libera di un semispazio elastico in presenza di fratture tensili, *Tesi di Laurea in Fisica* University of Bologna (in Italian).
- Davis, P.M., 1983. Surface deformation associated with a dipping hydrofracture, *J. geophys. Res.*, **88**, 5826–5834.
- Dieterich, J.H. & Decker, R.W., 1975. Finite element modelling of surface deformation associated with volcanism, *J. geophys. Res.*, **80**, 4094–4102.
- Erdogan, F., Gupta, G.D. & Cook, T.S., 1973. Numerical solution of singular integral equations, in *Mechanics of Fracture*, Vol. I, pp. 368–425, ed. Sih, G.C., Noordhoff, The Netherlands.
- Kannigieser, E., 1983. Vertical component of ground deformation in northern Iceland, *Ann. Geophys.*, **1**, 321–328.
- Kushiro, I., 1980. Viscosity density and structure of silicate melts at high pressures and their petrological applications, in *Physics of Magmatic Processes*, pp. 93–117, ed. Hargraves, R.B., Princeton University Press, Princeton, NJ.
- Landau, L. & Lifchitz, E., 1967. *Théorie de l'élasticité*, MIR, Moscow.
- Lister, J.R., 1990. Buoyancy-driven fluid fracture: the effects of material toughness and of low viscosity precursors, *J. Fluid. Mech.*, **210**, 263–280.
- Lister, J.R., 1991. Steady solutions for feeder dykes in a density-stratified lithosphere, *Earth planet. Sci. Lett.*, **107**, 233–242.
- Mindlin, R.D., 1936. Force at a point in the interior of a semi-infinite solid, *Physics*, **7**, 195–202.
- Murray, J.B., 1990. High level magma transport at Mt Etna volcano as deduced from ground deformation measurements, in *Magma Transport and Storage*, pp. 357–383, ed. Ryan, M.P., J. Wiley & Sons, New York.
- Murray, J.B., 1994. Elastic model of the actively intruded dyke feeding the 1991–93 eruption of Mt Etna derived from ground deformation measurements, *Acta Vulcanol.*, **4**, 97–99.
- Muskhelishvili, N.I., 1953. *Singular integral equation*, Noordhoff, Groningen.
- Pollard, D.D. & Holzhausen, G., 1979. On the mechanical interaction between a fluid-filled fracture and the earth's surface, *Tectonophysics*, **53**, 27–57.
- Pollard, D.D., Delaney, P.T., Duffield, W.A., Endo, E.T. & Okamura, A.T., 1983. Surface deformation in volcanic rift zones, *Tectonophysics*, **94**, 541–584.
- Rymer, H., Murray, J.B., Brown, G.C., Ferrucci, F. & McGuire, W.J., 1993. Mechanism of magma eruption and emplacement at Mt Etna between 1989 and 1992, *Nature*, **361**, 493–441.
- Rymer, H., Brown, G.C., Ferrucci, F. & Murray, J.B., 1994. Dyke intrusion mechanisms on Etna 1989–93 and microgravity precursors to eruption, *Acta Vulcanol.*, **4**, 109–114.
- Spence, D.A. & Turcotte, D.L., 1985. Magma-driven propagation of crack, *J. geophys. Res.*, **90**, 575–580.
- Turcotte, D.L. & Schubert, G., 1982. *Geodynamics, Applications of Continuum Physics to Geological Problems*, Wiley, New York.